

Synthesis, Characterization, and Photocontrolled Ring-Opening Polymerization of Sila[1]ferrocenophanes with Multiple Alkyne Substituents

Wing Yan Chan,[†] Alan J. Lough,[†] and Ian Manners^{*,†,‡}

Department of Chemistry, University of Toronto, 80 St. George Street, Toronto, Ontario, Canada, M5S 3H6, and the School of Chemistry, University of Bristol, Bristol, England, B58 ITS

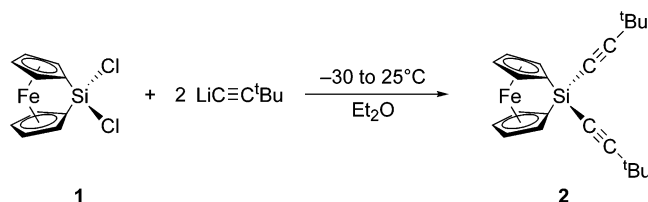
Received August 23, 2006

Sila[1]ferrocenophanes with multiple alkyne substituents [Fe(η -C₅H₄)₂Si(C≡C^tBu)₂] (**2**) and [Fe(η -C₅H₄)₂Si(Me)C≡CC≡CPh] (**5**) have been synthesized and structurally characterized. These compounds are prepared by reacting [LiC≡C^tBu] or [LiC≡CC≡CPh] with sila[1]ferrocenophanes containing silicon–chlorine bonds. Ring-opening polymerizations (ROP) of **2** and **5** have been studied using transition metal-catalyzed, thermal, anionic, and photocontrolled routes. Thermal and anionic ROP both failed to give significant amounts of polymer (<30%). And unlike most other ferrocenophanes, **2** cannot be polymerized by Karstedt's catalyst, possibly due to chelation of the catalyst by the acetylide ligands. Platinum-catalyzed ROP of **5** was also relatively ineffective, giving polymers with bimodal molecular weight distributions in moderate yields. Nevertheless, living polymerization of **2** and **5** was possible using photocontrolled ROP with NaCp as initiator. The key to photocontrolled ROP was the reduced basicity of NaCp compared to BuLi, as the latter reacted with the carbon–carbon triple bonds in the ferrocenophanes. Metal complexation of the triple bonds in **5** was also examined; this species reacted with [Co₂(CO)₈] to give [Fe(η -C₅H₄)₂Si(Me){Co₂(CO)₆C₂Co₂(CO)₆C₂Ph}] (**7**), a bimetallic ferrocenophane with five metal atoms.

Introduction

Metal-containing polymers have received increasing attention in recent years due to their unique properties and potential uses as functional materials.^{1,2} For example, polymetallaynes have shown interesting behavior such as lyotropic liquid crystallinity, optical nonlinearity, photoconductivity, and luminescence.^{3–5} Conjugated metallopolymers have been investigated for uses in electroluminescent and photosensitizing devices,⁶ as well as chemical and biological sensors.⁷ In addition to linear polymers, metal dendrimers⁸ are also of interest since incorporation of organometallic species into the core or the periphery of dendrimers imparts electroactivity, optical response, and catalytic properties,^{9,10} allowing the fabrication of sensors for gases and biomolecules.¹¹ Furthermore, metal-containing polymers have

Scheme 1. Synthesis of Ferrocenophane **2** with Two Acetylide Substituents



found applications as precursors to ceramics embedded with magnetic or catalytically active nanoparticles,^{12–14} lithographic resists,^{15,16} and supramolecular materials.^{17,18}

Polyferrocenylsilanes (PFS) represent a subset of polymetallocenes that have been extensively studied over the last decade. These materials are readily synthesized through ring-opening polymerization (ROP) of strained [1]ferrocenophanes using

* Corresponding author. E-mail: Ian.Manners@Bristol.ac.uk.

[†] University of Toronto.

[‡] University of Bristol.

(1) (a) Archer, R. D. *Inorganic and Organometallic Polymers*; John Wiley & Sons Inc: New York, 2001. (b) Abd-El-Aziz, A. S.; Harvey, P. D., Eds. *Macromol. Symp.* **2004**, *209*, 1–251.

(2) (a) Manners, I. *Science* **2001**, *294*, 1664–1666. (b) Manners, I. *Synthetic Metal-Containing Polymers*; Wiley-VCH: Weinheim, 2004.

(3) Long, N. J.; Williams, C. K. *Angew. Chem., Int. Ed.* **2003**, *42*, 2586–2617.

(4) Nguyen, P.; Gómez-Elipe, P.; Manners, I. *Chem. Rev.* **1999**, *99*, 1515–1548.

(5) Wong, W.-Y.; Lu, G.-L.; Choi, K.-H.; Shi, J.-X. *Macromolecules* **2002**, *35*, 3506–3513.

(6) Abd-El-Aziz, A. S.; Carraher, C. E., Pittman, C. U., Zeldin, M., Eds. *Metal-Coordination Polymers, Macromolecules Containing Metal and Metal-Like Elements*; John Wiley & Sons: New York, 2005; Vol. 5.

(7) Holliday, B. J.; Swager, T. M. *Chem. Commun.* **2005**, 23–36.

(8) Newkome, G. R.; He, E.; Moorefield, C. N. *Chem. Rev.* **1999**, *99*, 1689–1746.

(9) Geng, J.; Li, H.; Zhou, D.; Huck, W. T. S.; Johnson, B. F. G. *Polyhedron* **2006**, *25*, 585–590.

(10) Astruc, D.; Chardac, F. *Chem. Rev.* **2001**, *101*, 2991–3023.

(11) Chase, P. A.; Klein Gebbink, R. J. M.; van Koten, G. J. *Organomet. Chem.* **2004**, *689*, 4026–4054.

(12) MacLachlan, M. J.; Ginzburg, M.; Coombs, N.; Coyle, T. W.; Raju, N. P.; Greedan, J. E.; Ozin, G. A.; Manners, I. *Science* **2000**, *287*, 1460–1463.

(13) Berenbaum, A.; Ginzburg-Margau, M.; Coombs, N.; Lough, A. J.; Safa-Sefat, A.; Greedan, J. E.; Ozin, G. A.; Manners, I. *Adv. Mater.* **2003**, *15*, 51–55.

(14) Lastella, S.; Jung, Y. J.; Yang, H.; Vajtai, R.; Ajayan, P. M.; Ryu, C. Y.; Rider, D. A.; Manners, I. *J. Mater. Chem.* **2004**, *14*, 1791–1794.

(15) Johnson, B. F. G.; Sanderson, K. M.; Shephard, D. S.; Ozkaya, D.; Zhou, W.; Ahmed, H.; Thomas, M. D. R.; Gladden, L.; Mantle, M. *Chem. Commun.* **2000**, 1317–1318.

(16) Chan, W. Y.; Clendinning, S. B.; Berenbaum, A.; Lough, A. J.; Aouba, S.; Ruda, H. E.; Manners, I. *J. Am. Chem. Soc.* **2005**, *127*, 1765–1772.

(17) Lohmeijer, B. G. G.; Schubert, U. S. *Angew. Chem., Int. Ed.* **2002**, *41*, 3825–3829.

(18) Beck, J. B.; Rowan, S. J. *J. Am. Chem. Soc.* **2003**, *125*, 13922–13923.

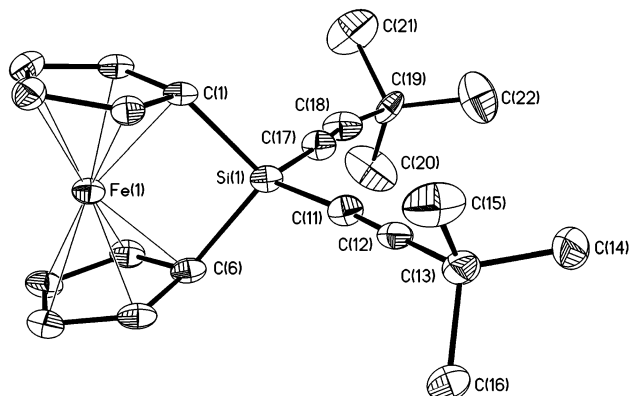


Figure 1. Molecular structure of **2** (thermal ellipsoids at 30% probability). Hydrogen atoms have been removed for clarity, and the disordered *tert*-butyl group (C19* to C22*) is not shown.

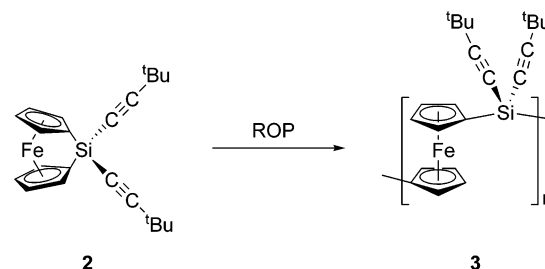
Table 1. Selected Bond Lengths (Å) and Angles (deg) for **2**

Si(1)–C(1)	1.881(4)	C(1)–Si(1)–C(6)	97.74(17)
Si(1)–C(6)	1.872(4)	C(11)–Si(1)–C(17)	114.31(19)
Si(1)–C(11)	1.815(4)	Si(1)–C(11)–C(12)	173.4(4)
Si(1)–C(17)	1.816(4)	C(11)–C(12)–C(13)	179.2(4)
C(11)–C(12)	1.215(5)	Si(1)–C(17)–C(18)	173.2(4)
C(12)–C(13)	1.466(5)	C(17)–C(18)–C(19)	166.3(5)
C(17)–C(18)	1.190(6)	α	19.26(24)
C(18)–C(19)	1.509(7)		
Fe(1)–Si(1)	2.6667(14)		

thermal,¹⁹ transition metal-catalyzed, and anionic routes.^{20,21} Recently, our group reported the photocontrolled living anionic ROP of sila[1]ferrocenophanes.^{22,23} In this method, UV excitation of the ferrocenophane monomer selectively weakens the iron–Cp bond, allowing the use of a mildly basic anion such as NaCp to initiate living polymerization. After the polymerization is quenched, PFS materials with narrow molecular weight distributions (PDI < 1.1) are obtained.²⁴

A current direction in our group is the development of synthetic strategies to increase the metal density in PFS to yield highly metallized polymers.²⁵ This can be achieved by introducing acetylide groups at the silicon atom of PFS to allow further reaction with transition metal complexes.²⁶ So far, clusters of

Scheme 2. Ring-Opening Polymerization of Ferrocenophane **2** to Give PFS **3**



Co, Mo, and Ni have been successfully introduced.^{16,27} The resulting highly metallized PFS have applications as precursors to magnetic nanoparticles^{28,29} and lithographic resists,^{16,30,31} and potentially for the fabrication of spintronic devices.³²

The presence of a second metal in the polymer (in addition to iron) imparts interesting properties to the material, allowing the patterning of silicon substrates on the microscale using electron-beam lithography and photolithography.¹⁶ Although the metallopolymers used in that study contained at least 25% metal by weight, it is still desirable for several applications to further increase the metal loading per repeat unit. This will allow access to a wider range of ratios between the two metals in the polymer, which is of interest in the systematic synthesis of Fe-containing bimetallic alloys. In addition, ceramics containing higher densities of metal nanoparticles should be accessible, which is potentially important for spintronic device applications.

One strategy to increase metal density is to add another carbon–carbon triple bond to the ferrocenophane for metal complexation. In principle, this might be achieved in two ways: (1) by using two acetylide substituents at silicon or (2) by the introduction of a conjugated diyne substituent at silicon. In this paper, we sequentially discuss each of these approaches.

Results and Discussion

Synthesis and Characterization of a Sila[1]ferrocenophane with Two Acetylenic Substituents (2). Sila[1]ferrocenophane **2** containing two acetylide substituents at silicon was synthesized by reacting ferrocenophane **1**, containing a SiCl₂ bridge, with lithium *tert*-butyl acetylide (Scheme 1).^{26,33}

After multiple recrystallizations from a mixture of toluene and hexanes, sila[1]ferrocenophane **2** was isolated in 21% yield³⁴ as a red-orange powder. Its ¹H NMR spectrum contained only one Cp resonance at δ 4.41 ppm, as the α - and β -protons are coincidental, and the methyl resonance was found at δ 1.11 ppm.

(19) Foucher, D. A.; Tang, B. Z.; Manners, I. *J. Am. Chem. Soc.* **1992**, *114*, 6246–6248.

(20) Ni, Y.; Rulkens, R.; Manners, I. *J. Am. Chem. Soc.* **1996**, *118*, 4102–4114.

(21) Manners, I. *Chem. Commun.* **1999**, 857–865.

(22) Tanabe, M.; Manners, I. *J. Am. Chem. Soc.* **2004**, *126*, 11434–11435.

(23) Tanabe, M.; Vandermeulen, G. W. M.; Chan, W. Y.; Cyr, P. W.; Vanderark, L.; Rider, D. A.; Manners, I. *Nat. Mater.* **2006**, *5*, 467–470.

(24) Prior work by Miyoshi and co-workers has shown that photolytic polymerization of phosphorus-bridged [1]ferrocenophanes in THF without an anionic initiator is also possible; however, the molecular weight distribution is considerably more broad (PDI > 1.6) and the system is not living. See: Mizuta, T.; Onishi, M.; Miyoshi, K. *Organometallics* **2000**, *19*, 5005–5009. Mizuta, T.; Imamura, Y.; Miyoshi, K. *J. Am. Chem. Soc.* **2003**, *125*, 2068–2069.

(25) Selected examples of highly metallized polymers and dendrimers: (a) Johnson, B. F. G.; Sanderson, K. M.; Shephard, D. S.; Ozkaya, D.; Zhou, W.; Ahmed, H.; Thomas, M. D. R.; Gladden, L.; Mantle, M. *Chem. Commun.* **2000**, 1317–1318. (b) Humphrey, M. G. *Macromol. Symp.* **2004**, *209*, 1–21. (c) Miinea, L. A.; Sessions, L. B.; Ericson, K. D.; Glueck, D. S.; Grubbs, R. B. *Macromolecules* **2004**, *37*, 8967–8972. (d) Sicard, S.; Bérubé, J.-F.; Samar, D.; Messaoudi, A.; Fortin, D.; Lebrun, F.; Fortin, J.-F.; Decken, A.; Harvey, P. D. *Inorg. Chem.* **2004**, *43*, 5321–5334. (e) Li, Z.; Dong, Y.; Qin, A.; Lam, J. W. Y.; Dong, Y.; Yuan, W.; Sun, J.; Hua, J.; Wong, K. S.; Tang, B. Z. *Macromolecules* **2006**, *39*, 467–469. (f) Scholz, S.; Leech, P. J.; Englert, B. C.; Sommer, W.; Weck, M.; Bunz, U. H. F. *Adv. Mater.* **2005**, *17*, 1052–1056.

(26) Berenbaum, A.; Lough, A. J.; Manners, I. *Organometallics* **2002**, *21*, 4415–4424.

(27) Chan, W. Y.; Berenbaum, A.; Clendenning, S. B.; Lough, A. J.; Manners, I. *Organometallics* **2003**, *22*, 3796–3808.

(28) Clendenning, S. B.; Han, S.; Coombs, N.; Paquet, C.; Rayat, M. S.; Grozea, D.; Brodersen, P. M.; Sodhi, R. N. S.; Yip, C. M.; Lu, Z.-H.; Manners, I. *Adv. Mater.* **2004**, *16*, 291–296.

(29) Liu, K.; Clendenning, S. B.; Friebe, L.; Chan, W. Y.; Zhu, X. B.; Freeman, M. R.; Yang, G. C.; Yip, C. M.; Grozea, D.; Lu, Z.-H.; Manners, I. *Chem. Mater.* **2006**, *18*, 2591–2601.

(30) Cheng, A. Y.; Clendenning, S. B.; Yang, G.; Lu, Z.-H.; Yip, C. M.; Manners, I. *Chem. Commun.* **2004**, 780–781.

(31) Clendenning, S. B.; Aouba, S.; Rayat, M. S.; Grozea, D.; Sorge, J. B.; Brodersen, P. M.; Sodhi, R. N. S.; Lu, Z.-H.; Yip, C. M.; Freeman, M. R.; Ruda, H. E.; Manners, I. *Adv. Mater.* **2004**, *16*, 215–219.

(32) Theoretical calculations by M. B. A. Jalil indicated that a nanogranular-in-gap structure can be used as a magnetic field-controlled nanoswitch: Jalil, M. B. A. *IEEE Trans. Magn.* **2002**, *38*, 2613–2615.

(33) The phenyl analogue of **2** was previously reported (see ref 26). We have changed the pendent substituent to *tert*-butyl to promote solubility of the resulting polyferrocenylsilane.

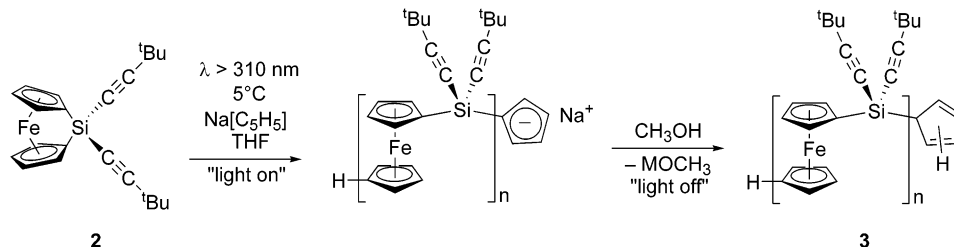
(34) As **2** is extremely soluble in toluene and hexanes, repeated recrystallizations (to remove traces of unidentified impurities) resulted in its reduced yield.

Table 2. Attempts at ROP of Monomer 2 to Give PFS 3

ROP method	catalyst/initiator	reaction conditions	conversion to polymer/isolated yield	M_n^a
TM-cat.	Karstedt's	21.5 h, 50 °C	0% conversion	
TM-cat.	PtCl ₂	2.5 h, 25 °C	100% conversion	gel
TM-cat.	PtCl ₂ ^b	5 h, 25 °C	40% yield	bimodal ^c
thermal (solution)	none	24 h, 160 °C in xylenes	20% conversion	
thermal (solution)	none	24 h, 175 °C in mesitylene	30% conversion	
thermal (bulk)	none	1 h, 185 °C	15% yield	trimodal ^c
anionic	ⁿ BuLi	-78 °C to 25 °C	multiple uncharacterized products	
photocontrolled	NaCp	1.5 h, 5 °C	80% yield	9.6 × 10 ³ (1.15)

^a The polydispersity index is given in parentheses. ^bEt₃SiH (ranging from 0.05 to 0.5 equiv) was added. ^cSee Experimental Section for detailed molecular weight distributions.

Scheme 3. Photocontrolled Living Ring-Opening Polymerization of Ferrocenophane 2 to Give PFS 3



The ¹³C NMR spectrum of **2** showed two Cp resonances at δ 78.2 and 75.6 ppm, and the *ipso*-Cp resonance at δ 29.9 ppm. A dramatic upfield shift of the *ipso*-Cp resonance from that of ferrocene (ca. δ 70 ppm) is typical for ferrocenophanes, as the Cp ligands are tilted toward each other to form a strained structure. The ²⁹Si NMR spectrum of **2** showed a single resonance at δ -55.3 ppm.

The molecular structure of **2** was confirmed using single-crystal X-ray crystallography. Figure 1 is the ORTEP diagram of **2**, and Table 1 lists pertinent bond lengths and angles for this compound.

The molecular structure of **2** confirmed the expected atom connectivity. The tilt angle (α) of 19.26(24)^o between the two Cp rings is typical for sila[1]ferrocenophanes. The carbon-carbon triple bond lengths in **2** are 1.215(5) Å (C(11)-C(12)) and 1.190(6) Å (C(17)-C(18)), respectively. These distances are comparable to that of the triple bond in free acetylene (1.20 Å).³⁵ The Fe-Si distance of 2.6667(14) Å in **2** also falls within the normal range of sila[1]ferrocenophanes (cf. $d(\text{Fe-Si}) = 2.55\text{--}2.75$ Å).^{36,37} The two alkynes in **2** are almost linear, with bond angles around the acetylenic carbons ranging from 166.3(5)^o to 179.2(4)^o. The geometric parameters of **2** are similar to those of its phenyl analogue.²⁶

Ring-Opening Polymerization of Sila[1]ferrocenophane 2 to Give Polyferrocenylsilane 3. We attempted the ROP of **2** under various conditions (Scheme 2 and Table 2). We began by using Karstedt's catalyst to induce ROP; however, this route failed to give polymer at either 25 or 50 °C. This may be a consequence of the coordination of Pt by both acetylide groups in **2**, thereby deactivating the catalyst.³⁸ When PtCl₂ was used as an alternate catalyst in toluene, an orange gel was formed after 2.5 h at 25 °C, suggesting the formation of very high molecular weight and/or cross-linked polymer. We have previously demonstrated the use of Et₃SiH for polymer molecular weight control in the Pt-catalyzed ROP of ferrocenophanes.³⁹ When Et₃SiH was added to the polymerization of **2** with PtCl₂, PFS **3** with a bimodal molecular weight distribution was consistently obtained in less than 50% yield.⁴⁰ Next, we tried refluxing a xylenes or mesitylene solution of **2** to induce thermal ROP, but the reaction was sluggish (maximum 30% conversion

after 24 h) in both cases. Thermal ROP of **2** in bulk at 185 °C was also unproductive, as it gave a gel and only a small amount of soluble polymer. When we attempted to ring-open **2** using a stoichiometric amount of ⁿBuLi in order to test the feasibility of anionic ROP, we observed multiple Cp and methyl resonances in the ¹H NMR spectrum of the product, suggesting the acetylide groups do not tolerate such a strong base. The synthesis of well-defined PFS **3** was finally achieved using photocontrolled ROP. In this method, NaCp was used as an anionic initiator to polymerize a photoactivated ferrocenophane at 5 °C.^{22,23} In contrast to the situation with ⁿBuLi, the less basic NaCp initiator is compatible with the acetylide substituents in **2**, allowing the preparation of soluble bis(acetylide)-substituted PFS **3** with a narrow, monomodal molecular weight distribution in 80% isolated yield (Scheme 3).

PFS **3** was fully characterized by NMR spectroscopy. Compared to that of **2**, the ¹H NMR spectrum of **3** showed downfield shifts of both Cp resonances (to δ 4.91 and 4.67 ppm) and the methyl resonance (to δ 1.23 ppm). As the Cp ligands are no longer tilted in PFS **3**, the *ipso*-Cp carbon resonance was found at δ 68.0 ppm, much closer to the ¹³C resonance of ferrocene (ca. δ 70 ppm). As expected, the ²⁹Si NMR signal of **3** at δ -46.0 is shifted downfield from that of **2** (δ -55.3 ppm). GPC analysis of **3** gave $M_n = 9600$ and PDI = 1.15, indicating

(35) Elschenbroich, C.; Salzer, A. *Organometallics: A Concise Introduction*; VCH Publishers Inc.: New York, 1992.

(36) Pudelski, J. K.; Foucher, D. A.; Honeyman, C. H.; Lough, A. J.; Manners, I.; Barlow, S.; O'Hare, D. *Organometallics* **1995**, *14*, 2470-2479.

(37) Zechel, D. L.; Hultsch, K. C.; Rulkens, R.; Balaishis, D.; Ni, Y.; Pudelski, J. K.; Lough, A. J.; Manners, I.; Foucher, D. A. *Organometallics* **1996**, *15*, 1972-1978.

(38) When we reacted monomer **2** with Karstedt's catalyst in a stoichiometric reaction, we observed the complete conversion of monomer **2** to various unidentified products (by ¹H NMR) after 3 h at 25 °C.

(39) (a) Gómez-Elipe, P.; Resendes, R.; Macdonald, P. M.; Manners, I. *J. Am. Chem. Soc.* **1998**, *120*, 8348-8356. (b) Temple, K.; Jäkle, F.; Sheridan, J. B.; Manners, I. *J. Am. Chem. Soc.* **2001**, *123*, 1355-1364.

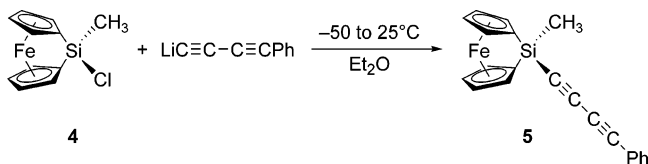
(40) A typical bimodal GPC trace contains a peak at $M_n \approx 5000\text{--}30\,000$ (ca. 90% of all polymer) and a higher molecular weight peak at $M_n \approx 10^6\text{--}10^7$ (ca. 10% of all polymer). Molecular weights of the polymer formed varied depending on the amount of PtCl₂ and Et₃SiH used, but all molecular weight distributions were bimodal.

Table 3. Photocontrolled ROP of 2 to Give PFS 3^a

[M]:[I]	time (h)	isolated yield of 3 (%)	M_n expected	M_n found ^b	PDI
25:1	2	83	9400	9400	1.11
50:1	2	89	18 700	24 100	1.11
75:1	4	88	28 100	43 100	1.15

^a Irradiations were performed at 5 °C with THF as solvent. ^b Molecular weights relative to polystyrene standards.

Scheme 4. Synthesis of Ferrocenophane 5 with a Diyne Substituent



the polymer was essentially monodisperse and possessed a well-defined microstructure.

We briefly explored the possibility of molecular weight control in the photocontrolled ROP of 2. Three monomer to initiator ratios were studied, and the results are summarized in Table 3. In all three experiments, monomodal PFS 3 with narrow molecular weight distributions was obtained in good yields. The low PDI values indicate this is a living polymerization.

Synthesis and Characterization of a Sila[1]ferrocenophane with a Diyne Substituent (5). Next, we investigated the second strategy to increase metal loading, i.e., introduction of a diyne substituent at silicon. Sila[1]ferrocenophane 5, containing a conjugated diyne, was synthesized by substitution of chloro-substituted sila[1]ferrocenophane 4 with the appropriate lithium salt (Scheme 4). After recrystallization from a mixture of toluene and hexanes, monomer 5 was isolated in 40% yield⁴¹ as a red solid. The ¹H NMR spectrum of 5 showed four multiplets in the Cp region (δ 4.41 to 3.81 ppm), typical for a ferrocenophane with asymmetric substitution at silicon. The *ipso*-Cp carbon resonance of 5 was found at δ 29.1 ppm, comparable to that of monomer 2 (cf. δ 29.9 ppm). The ²⁹Si NMR spectrum of 5 contained a single resonance at δ -26.9 ppm.

A single-crystal X-ray diffraction study was performed to confirm the molecular structure of 5. Figure 2 shows the ORTEP diagram of 5, and Table 4 contains a summary of geometric parameters.

The molecular structure of 5 was as expected.⁴² The tilt angle (21.04(24)°) and Fe–Si distance (2.6961(12) Å) of 5 are comparable to those of 2 (cf. α = 19.26(24)°, $d(\text{Fe}–\text{Si})$ = 2.6667(14) Å). Also, carbon–carbon bond lengths in the diyne substituent alternate between that of a single bond (1.384(5) to 1.437(5) Å) and a triple bond (1.201(5) to 1.203(5) Å). As in 2, the carbon–carbon triple bonds in 5 are approximately linear, and bond angles around the acetylenic carbons range from 175.8(4)° to 178.6(4)°.

Ring-Opening Polymerization of Sila[1]ferrocenophane 5 to Give Polyferrocenyloxysilane 6. Although some conjugated diynes have been known to polymerize in a topochemical 1,4-addition in the solid state upon exposure to heat, UV–visible light, or γ -rays,⁴³ monomer 5 is stable when stored at 25 °C in

(41) The rather low yield of 5 is a consequence of the reduced purity of PhC≡CCl, as not all of 4 is consumed in the reaction depicted in Scheme 3.

(42) There are two independent molecules of 5 in an asymmetric unit of the crystal lattice, but their bond lengths and bond angles are identical within experimental error. Geometric parameters quoted in the article are that of one independent molecule.

(43) Enkelmann, V. *Chem. Mater.* **1994**, *6*, 1337–1340.

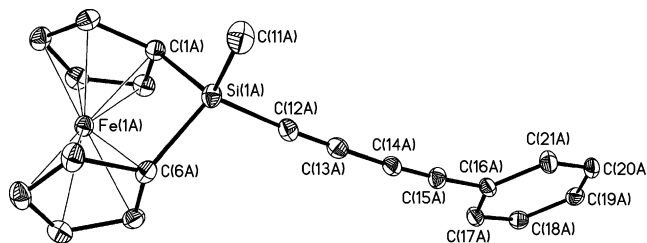
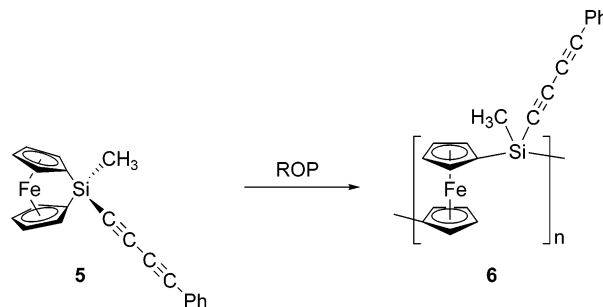


Figure 2. Molecular structure of 5 (thermal ellipsoids at 30% probability). Hydrogen atoms have been removed for clarity, and only one of the two independent molecules of 5 in an asymmetric unit is shown.

Table 4. Selected Bond Lengths (Å) and Angles (deg) for 5

Si(1A)–C(1A)	1.885(4)	C(1A)–Si(1A)–C(6A)	96.42(16)
Si(1A)–C(6A)	1.879(4)	C(11A)–Si(1A)–C(12A)	110.03(19)
Si(1A)–C(12A)	1.827(4)	Si(1A)–C(12A)–C(13A)	176.7(3)
C(12A)–C(13A)	1.203(5)	C(12A)–C(13A)–C(14A)	178.6(4)
C(13A)–C(14A)	1.384(5)	C(13A)–C(14A)–C(15A)	176.7(5)
C(14A)–C(15A)	1.201(5)	C(14A)–C(15A)–C(16A)	175.8(4)
C(15A)–C(16A)	1.437(5)	α	21.04(24)
Fe(1A)–Si(1A)	2.6961(12)		

Scheme 5. Ring-Opening Polymerization of Ferrocenophane 5 to Form PFS 6



an inert atmosphere glovebox. An inspection of the unit cell of 5 reveals that the diyne substituents of adjacent monomers are probably not packed closely enough for polymerization to take place in the solid state.⁴⁴ We then attempted to deliberately polymerize 5 using various methods. Beginning with transition metal-catalyzed ROP, we used Karstedt's catalyst and Et₃SiH for molecular weight control. We were successful in forming PFS 6_{Karstedt's} in 50% yield (Scheme 5). In contrast to monomer 5, no polymer was formed when Karstedt's catalyst was used to polymerize monomer 2. This difference in reactivity is likely due to the varying geometry of the two carbon–carbon triple bonds in the ferrocenophanes. In monomer 2, the two alkynes are positioned such that they can chelate a metal ion; however, the two triple bonds in monomer 5 are conjugated in a linear fashion and chelate formation is not possible. As a result, the behavior of monomer 5 in Karstedt's-catalyzed ROP mirrors that of ferrocenophanes with one acetylide substituent at the silicon (they readily polymerize),²⁶ but monomer 2 does not.

The highly asymmetrical substitution at the silicon atom of monomer 5 offers the possibility of forming a stereoregular polymer, as the steric demands of the methyl and diyne substituents are significantly different. We therefore investigated the effects of ROP protocols on the microstructure of PFS 6. The ¹H NMR spectrum of PFS 6_{Karstedt's} synthesized using Karstedt's catalyst shows a broad methyl resonance at δ 0.75 ppm, clearly indicating that the polymer was not stereoregular. GPC analysis of PFS 6_{Karstedt's} also showed that the molecular

(44) Diyne monomers need to be spaced at 4.9 Å with a 45° declination angle; see ref 43 for details.

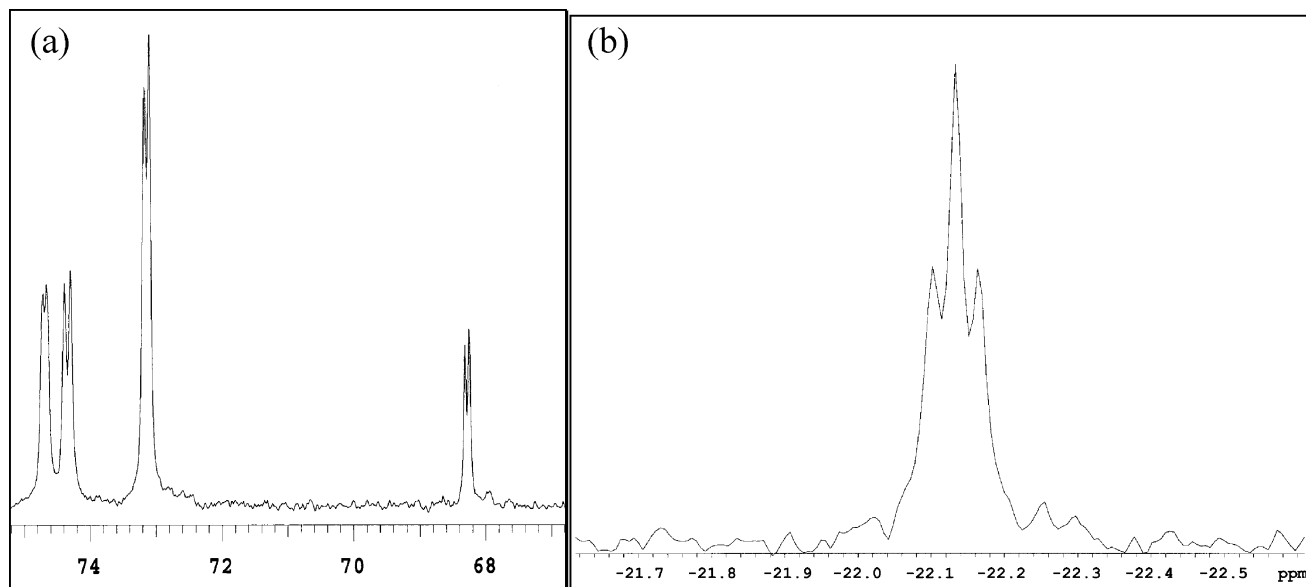
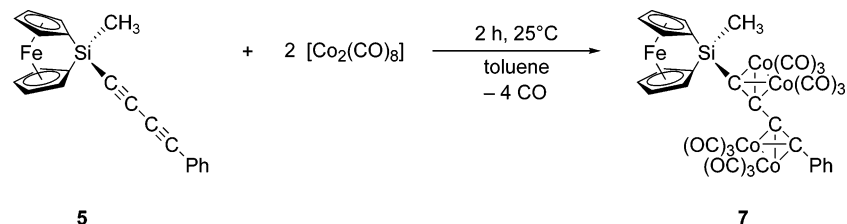


Figure 3. (a) 100 MHz $^{13}\text{C}\{^1\text{H}\}$ NMR spectrum of PFS $\mathbf{6}_{\text{PtCl}_2}$ (expansion of Cp region). (b) 79.4 MHz $^{29}\text{Si}\{^1\text{H}\}$ NMR spectrum of PFS $\mathbf{6}_{\text{PROP}}$.

Scheme 6. Clusterization of Ferrocenophane 5 with $[\text{Co}_2(\text{CO})_8]$ to Give Ferrocenophane 7



weight distribution was bimodal. When PtCl_2 was used as an alternate catalyst for transition metal-catalyzed ROP, PFS $\mathbf{6}_{\text{PtCl}_2}$ was formed in 78% yield and the ^1H NMR spectrum of this sample also contained a methyl resonance at δ 0.75 ppm. The Cp resonances of PFS $\mathbf{6}_{\text{PtCl}_2}$ occur in pairs in the ^{13}C NMR spectrum, showing dyad resolution for an atactic polymer (Figure 3a). However, the molecular weight distribution of PFS $\mathbf{6}_{\text{PtCl}_2}$ was broad and bimodal (fraction 1: $M_n = 3.8 \times 10^6$, PDI = 1.81, 15%; fraction 2: $M_n = 4.0 \times 10^4$, PDI = 3.05, 85%). Thermal ROP of **5** was also attempted: when performed in either refluxing xylenes or mesitylene, a gel was obtained after 1 h of heating, suggesting the formation of very high molecular weight and/or cross-linked polymer. In the case of xylenes, a small amount of soluble PFS $\mathbf{6}_{\text{xylenes}}$ was isolated

Table 5. Selected Bond Lengths (\AA) and Angles (deg) for $7 \cdot 0.5\text{C}_7\text{H}_8$

Si(1)–C(1)	1.887(5)	C(1)–Si(1)–C(6)	96.8(2)
Si(1)–C(6)	1.888(5)	Si(1)–C(12)–C(13)	149.9(4)
C(12)–C(13)	1.350(6)	C(12)–C(13)–C(21)	141.8(4)
C(13)–C(21)	1.435(6)	C(13)–C(21)–C(20)	143.1(4)
C(20)–C(21)	1.362(5)	C(21)–C(20)–C(28)	140.8(4)
Co(1)–Co(2)	2.4489(9)	α	19.54(28)
Co(3)–Co(4)	2.4693(9)		
Fe(1)–Si(1)	2.6848(15)		

(13% yield), and its ^1H and ^{13}C NMR spectra were very similar to those of PFS $\mathbf{6}_{\text{PtCl}_2}$, again suggesting the formation of an atactic polymer. Next, we tried photocontrolled ROP of **5** with NaCp as initiator. After 2 h of photolysis, PFS $\mathbf{6}_{\text{PROP}}$ was isolated in 87% yield following precipitation into hexanes. In contrast to the polymers from thermal and metal-catalyzed ROP, the ^1H NMR spectrum of this sample contained sharp signals and a single methyl resonance at δ = 0.74 ppm. Furthermore, its ^{29}Si NMR spectrum showed a well-resolved 3 line pattern due to triad resolution in an approximate 1:2:1 ratio centered at δ = –22.1 ppm, suggesting the polymer is atactic (Figure 3b).³⁷ GPC analysis also confirmed that PFS $\mathbf{6}_{\text{PROP}}$ is well-defined with a narrow molecular weight distribution ($M_n = 8400$, PDI = 1.10). Comparing all the polymerization methods, photocontrolled ROP of **5** gave PFS **6** with the most narrow molecular weight distribution; however, none of the routes gave a stereoregular polymer.

Clusterization of the Triple Bond in Sila[1]ferrocenophane 5 Using $[\text{Co}_2(\text{CO})_8]$. As one of the goals of this research is to further increase the metal content of highly metallized PFS, we want to confirm that the clusterization reactions we have previously developed²⁷ will apply to the diyne-substituted sila-

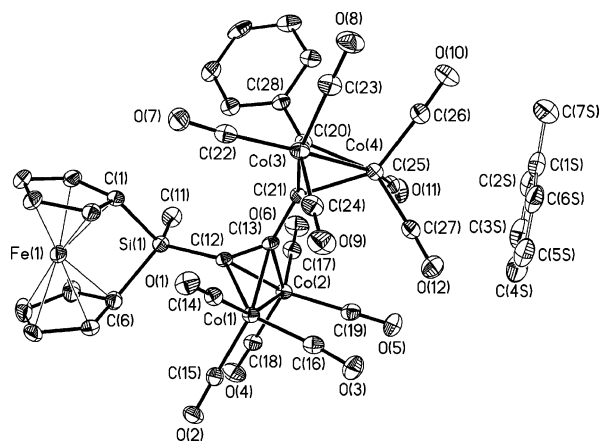


Figure 4. Molecular structure of $7 \cdot 0.5\text{C}_7\text{H}_8$ (thermal ellipsoids at 30% probability). Hydrogen atoms have been omitted for clarity.

Table 6. Selected Crystal, Data Collection, and Refinement Parameters for **2**, **5**, and **7·0.5C₇H₈**

	2	5	7·0.5C₇H₈
formula	C ₂₂ H ₂₆ FeSi	C ₂₁ H ₁₆ FeSi	C ₃₃ H ₁₆ Co ₄ FeO ₁₂ Si·0.5C ₇ H ₈
<i>M_r</i>	374.37	352.28	970.19
cryst syst	monoclinic	orthorhombic	triclinic
space group	<i>P2(1)/c</i>	<i>Pca2₁</i>	<i>P1</i>
color	orange-red	red	dark brown
<i>a</i> , Å	14.4265(3)	19.0405(5)	8.8609(4)
<i>b</i> , Å	12.7510(5)	7.5017(1)	9.3119(4)
<i>c</i> , Å	11.5855(5)	23.3594(6)	22.3450(8)
α, deg	90	90	83.815(3)
β, deg	106.64(3)	90	83.552(3)
γ, deg	90	90	85.989(2)
<i>V</i> , Å ³	2041.92(13)	3336.57(13)	1818.27(13)
temperature, K	150(1)	150(1)	150(1)
<i>Z</i>	4	8	2
ρ _{calc} , g cm ⁻³	1.218	1.403	1.772
μ(Mo Kα), mm ⁻¹	0.797	0.971	2.273
<i>F</i> (000)	792	1456	966
cryst size, mm ³	0.10 × 0.10 × 0.10	0.34 × 0.12 × 0.04	0.22 × 0.16 × 0.05
θ range, deg	2.56–27.52	2.72–27.48	2.58–27.57
no. of reflns collected	17 865	19 318	21 552
no. of indep reflns	4668	6599	8201
	(<i>R</i> _{int} = 0.0974)	(<i>R</i> _{int} = 0.0565)	(<i>R</i> _{int} = 0.0973)
abs corr	semiempirical from equivalents		
max. and min. transmn coeff	0.927 and 0.863	0.967 and 0.755	0.893 and 0.694
no. of params refined	254	419	514
GoF on <i>F</i> ²	1.034	1.017	0.991
<i>R</i> 1 ^a (<i>I</i> > 2σ(<i>I</i>))	0.0557	0.0384	0.0521
w <i>R</i> 2 ^b (all data)	0.1589	0.0895	0.1402
Peak and hole, e Å ⁻³	0.576 and -0.454	0.448 and -0.497	0.592 and -0.820

[1]ferrocenophane.⁴⁵ We chose to test the reactivity of monomer **5** with [Co₂(CO)₈], as the complexation reaction should proceed at room temperature. When monomer **5** and [Co₂(CO)₈] were reacted in toluene for 2 h, both carbon–carbon triple bonds were transformed into Co₂C₂ clusters. After recrystallization from a mixture of toluene and hexanes, cobalt-clusterized ferrocenophane **7** was isolated in 62% yield as a dark brown solid (Scheme 6).

Upon clusterization of the diyne substituent, all ¹H NMR signals of **7** were found downfield from those of **5**. A similar shift was observed in the ¹³C NMR spectrum of **7**, as the *ipso*-Cp carbon resonance moved from δ 29.1 ppm in **5** to δ 33.2 ppm in **7**. The ²⁹Si NMR spectrum of **7** contained a singlet at δ -11.5 ppm, downfield from that of **5** (cf. δ -26.9 ppm). To confirm the molecular structure of **7**, a single-crystal X-ray diffraction study was performed. Figure 4 shows the ORTEP diagram of **7·0.5C₇H₈**, and Table 5 lists selected geometric parameters for this compound.

The molecular structure of **7·0.5C₇H₈** confirmed the expected atomic arrangement. Introduction of the cobalt clusters did not affect the tilt angle of the ferrocenophane, but bond distances in the diyne substituent have increased significantly. Upon clusterization, the carbon–carbon triple bonds lengthened from 1.201(5) Å to 1.362(5) Å, and the single bond lengthened from 1.384(5) Å to 1.435(6) Å. The conjugated diyne also changed from an almost linear to a bent geometry, with more acute bond angles around the carbon atoms in **7·0.5C₇H₈** (140.8(4)° to 149.9(4)°). These changes in bond length and angles in the diyne substituent upon clusterization are expected as the carbon atoms rehybridize from sp to approaching sp³. For the Co₂C₂ clusters, the cobalt–cobalt axes lie perpendicular to the carbon–carbon axes. The cobalt–cobalt bond distances in **7·0.5C₇H₈** are similar to those in other ferrocenophanes containing cobalt clusters.²⁷

Summary

We have synthesized two ferrocenophanes containing multiple carbon–carbon triple bonds in different geometric arrangements. Ferrocenophane **2** contains two acetylide substituents at silicon, while ferrocenophane **5** has a diyne substituent at silicon. The geometry of the triple bonds affects the polymerization behavior of these ferrocenophanes. For example, the two carbon–carbon triple bonds in ferrocenophane **2** could form a chelate with an incoming metal catalyst, apparently deactivating the Karstedt's catalyst in transition metal-catalyzed ROP. Hence, monomer **2** could only be polymerized to give well-defined PFS **3** using photocontrolled ROP. In contrast to monomer **2**, monomer **5** contains two conjugated carbon–carbon triple bonds. Since chelate formation is not possible with ferrocenophane **5**, it can be polymerized using Karstedt's catalyst to give PFS **6**. Preparation of PFS **6** with a narrow molecular weight distribution was possible through photocontrolled ROP; the polymer formed was atactic and not stereoregular. It is significant that photocontrolled ROP allowed the living polymerizations of monomers **2** and **5** to give materials with narrow molecular weight distributions when living anionic ROP using BuLi failed. Both PFS **3** and **6** are important precursors to highly metalized PFS, as they allow the incorporation of up to five metal atoms per polymer repeat unit.

We have also explored metal complexation of the diyne substituent in ferrocenophane **5**. Reaction of **5** with [Co₂(CO)₈] resulted in clusterization of both carbon–carbon triple bonds and the formation of bimetallic ferrocenophane **7** in 62% yield. We are currently studying the metal complexation of PFSs **3** and **6** and pyrolysis of the resulting materials to form ceramics.⁴⁶

Experimental Section

ⁿBuLi (1.6 M in hexanes), ^tBuC≡CH, (CH₃)₃SiCl, Et₃SiH, NaCp (2 M in THF), and PhC≡CH were purchased from Aldrich. ^tBuC≡

(45) Previous clusterization experiments of bis(acetylide)-substituted ferrocenophanes using [Co₂(CO)₈] revealed that the products have a tendency to spontaneously ring-open to give a silanol. See ref 27 for details.

(46) For preliminary results of the metal complexation experiments, see ref 23.

CH was dried over 4 Å molecular sieves, and Et₃SiH, (CH₃)₃SiCl, and PhC≡CH were distilled before use. [Co₂(CO)₈] was purchased from STREM and sublimed immediately before use. Reactions involving [Co₂(CO)₈] required ambient light to proceed. Karstedt's catalyst (platinum–divinyltetramethyldisiloxane complex, 2.1–2.4 wt % Pt in xylenes) was purchased from Gelest and used as received. PtCl₂ was purchased from Pressure Chemicals and used as received. Compounds **1**,³⁷ **4**,³⁷ and HC≡CC≡CPh⁴⁷ were synthesized according to literature procedures. Deprotonation of HC≡CC≡CPh with ⁿBuLi in Et₂O gave LiC≡CC≡CPh.

Most reactions and manipulations were performed under an atmosphere of prepurified N₂ using Schlenk techniques or in an inert atmosphere glovebox. Unless specified as ACS grade, solvents were dried using the Grubbs method⁴⁸ or standard methods followed by distillation. The air- and moisture-stable polymers **3** and **6** were handled in air with ACS grade solvents after workup. ¹H (400 MHz), ¹³C (100.5 MHz), and ²⁹Si (79.4 MHz) NMR spectra were recorded on a Varian Unity 400 spectrometer. ¹H resonances were referenced internally to the residual protonated solvent resonances. ¹³C resonances were referenced internally to the deuterated solvent resonances, and ²⁹Si resonances were referenced externally to TMS. Molecular weights were determined by gel permeation chromatography (GPC) using a Viscotek GPC MAX liquid chromatograph equipped with a Viscotek triple detector array. The triple detector array consists of a deflection refractometer, a four-capillary differential viscometer, and a right angle laser light scattering detector (λ₀ = 670 nm). Conventional calibration was used and molecular weights were determined relative to polystyrene standards purchased from American Polymer Standards. A flow rate of 1.0 mL/min was used with ACS grade THF as the eluent. Electron impact (EI) mass spectra were recorded with a Micromass 70S-250 mass spectrometer in electron impact mode. The calculated isotopic distribution for each ion was in agreement with experimental values. Elemental analyses were performed using a Perkin-Elmer 2400 C/H/N analyzer. Ultraviolet–visible spectra were recorded using a Perkin-Elmer Lambda 900 UV/vis/NIR spectrometer. Photocontrolled polymerizations were carried out with a Philips HPK 125 high-pressure mercury-arc lamp. A Pyrex filter was placed inside the quartz immersion well to filter out wavelengths below 310 nm, and a thermostated water bath was used to maintain the reaction temperature at 5 °C.

Synthesis of 2. ⁿBuLi (1.6 M, 28.0 mL, 44.8 mmol) was added dropwise to an Et₂O solution (50 mL) of ^tBuC≡CH (5.9 mL, 47.9 mmol) at 0 °C. The solution was kept at 0 °C for 60 min, and it was added dropwise to a solution of **1** (6.02 g, 21.3 mmol) in Et₂O (200 mL) at –30 °C. The reaction mixture was allowed to warm to 25 °C and was stirred for a further 2 h. (CH₃)₃SiCl (10 drops) was added, and the orange suspension was stirred for 15 min. All volatile materials were removed in vacuo, and the orange residue was dried under vacuum overnight. Hexanes (5 × 75 mL) was then added, and the red solution was filtered through a glass frit to remove LiCl. The filtrate was concentrated in vacuo to give a red-orange solid. Recrystallization in toluene/hexanes (4:1) gave 3.85 g of **2** as a red-orange powder. Repeated recrystallizations using the same solvents gave highly purified **2**, yield 1.65 g (21%). This stringent purification protocol is necessary to obtain highly pure monomer for photocontrolled ROP reactions. Crystals suitable for X-ray crystallography were obtained from a toluene/hexanes (2:5) solution at –35 °C.

For 2: ¹H NMR (400 MHz, C₆D₆, 25 °C) δ 4.41 (br m, 8 H, Cp), 1.11 (s, 18 H, CH₃); ¹³C{¹H} NMR (100.5 MHz, C₆D₆, 25 °C) δ 118.7 (2 C, SiC≡C^tBu), 78.2 (4 C, Cp), 76.0 (2 C, SiC≡C^tBu), 75.6 (4 C, Cp), 30.6 (6 C, C(CH₃)₃), 29.9 (2 C, *ipso*-Cp), 28.5 (2 C, C(CH₃)₃); ²⁹Si{¹H} NMR (79.4 MHz, C₆D₆, 25 °C) δ

–55.3; MS (EI, 70 eV) *m/z* (%) 374 (64); HRMS (EI, 70 eV) calcd for C₂₂H₂₄⁵⁶FeSi 374.115319, found 374.116033, fit 1.9 ppm; UV–vis (25 °C, THF) λ_{max} = 482 nm, ε = 340 L·mol^{–1}·cm^{–1}.

Attempted ROP of 2 Using Karstedt's Catalyst. **2** (50 mg, 0.13 mmol) was dissolved in C₆D₆ (1 mL) in an NMR tube, and Karstedt's catalyst (5 μL) was added. The reaction was monitored by ¹H NMR spectroscopy and showed no changes after 3 h. The solution was then heated at 50 °C for 21.5 h, and a ¹H NMR spectrum taken at this point confirmed there was no reaction.

When this reaction was repeated in the presence of Et₃SiH (0.1 equiv), analysis of the mixture by ¹H NMR spectroscopy after 5 h at 25 °C showed 4% conversion to polymer.

Attempted ROP of 2 Using PtCl₂. **2** (50 mg, 0.13 mmol) was dissolved in toluene (1 mL) and a trace of PtCl₂ was added. An orange gel was obtained after 2.5 h of stirring. Addition of more toluene failed to completely dissolve the gel.

Transition Metal-Catalyzed ROP of 2 Using PtCl₂ in the Presence of Et₃SiH. **2** (201 mg, 0.54 mmol) was dissolved in toluene (4 mL), and Et₃SiH (4.3 μL, 0.027 mmol) was added. PtCl₂ (7 mg, 0.024 mmol) was added, and the suspension was stirred for 5 h. The suspension became orange and slightly viscous. Precipitation into rapidly stirred ACS grade MeOH (25 mL) gave a yellow gummy solid. It was washed three times with ACS grade MeOH and dried overnight under high vacuum, yield 85 mg (42%). GPC analysis revealed a bimodal molecular weight distribution: peak 1, *M_n* > 10⁶, 8%; peak 2, *M_n* = 7.3 × 10³, *M_w* = 2.3 × 10⁴, PDI = 3.11, 92%. The exact molecular weights of the two peaks depend on the amount of PtCl₂ and Et₃SiH used. Et₃SiH amounts ranging from 0.05 to 0.5 molar equiv (with respect to **2**) were tested, but the molecular weight distribution remains bimodal.

Attempted Thermal ROP of 2 in Solution. **2** (203 mg, 0.54 mmol) was dissolved in xylenes (4 mL), and the solution was heated at 160 °C. An aliquot was taken after 24 h, and analysis by ¹H NMR spectroscopy showed 20% conversion to polymer. When an analogous reaction was performed using mesitylene as solvent and heating at 175 °C, conversion of 30% was achieved after 24 h.

Attempted Thermal ROP of 2 in Bulk. **2** (196 mg, 0.52 mmol) was sealed inside an evacuated Pyrex tube and heated at 185 °C for 60 min until the molten solid was no longer free flowing. ACS grade THF (2 mL) was used to extract soluble materials from the solid, but a gel was formed. The soluble fraction was precipitated into ACS grade MeOH (75 mL) to give a fine yellow powder. Centrifugation of the suspension followed by drying under high vacuum gave a light brown solid, yield 30 mg (15%). ¹H NMR analysis of the brown solid showed the presence of polymer. GPC analysis of the brown solid revealed a trimodal distribution: peak 1, *M_n* > 10⁶, 13%; peak 2, *M_n* = 3.0 × 10⁵, *M_w* = 1.8 × 10⁶, PDI = 5.91, 82%; peak 3, *M_n* = 2.9 × 10³, *M_w* = 6.0 × 10³, PDI = 2.04, 5%.

Attempted Ring-Opening of 2 Using a Stoichiometric Amount of ⁿBuLi. **2** (100 mg, 0.27 mmol) was dissolved in THF (1 mL), and the red solution was cooled to –78 °C for 10 min. ⁿBuLi (0.17 mL of 1.6 M solution, 0.27 mmol) was added dropwise, and the solution was allowed to warm to 25 °C. (CH₃)₃SiCl (0.1 mL) was added to the brown solution, and the solution was concentrated to dryness to give an oil. The ¹H NMR spectrum of the residue showed multiple broad resonances at δ 4.9–4.1, 1.8–0.8, and 0.4–0.1 ppm.

Photocontrolled ROP of 2 to Give PFS 3. In the absence of light, **2** (100 mg, 0.27 mmol) was dissolved in THF (2 mL) in a Schlenk tube, and NaCp (2 M, 6.7 μL, 0.014 mmol) was added using a microsyringe. The solution was photolyzed at 5 °C for 1.5 h, and the color changed from dark red to orange. Five drops of degassed, ACS grade MeOH was added, and the solution was stirred for 5 min. The orange solution was precipitated into rapidly stirred ACS grade MeOH (50 mL) to give a yellow, fluffy solid. Filtration through a fritted glass funnel followed by drying under high vacuum gave PFS **3** as a pale yellow solid, yield 80 mg (80%).

(47) Kende, A. S.; Smith, C. A. *J. Org. Chem.* **1988**, *53*, 2655–2657.

(48) Pangborn, A. B.; Giardello, M. A.; Grubbs, R. H.; Rosen, R. K.; Timmers, F. J. *Organometallics* **1996**, *15*, 1518–1520.

For **3**: ^1H NMR (400 MHz, C_6D_6 , 25 °C) δ 4.91 (br m, 4 H, Cp), 4.67 (br m, 4 H, Cp), 1.23 (s, 18 H, CH_3); $^{13}\text{C}\{^1\text{H}\}$ NMR (100.5 MHz, C_6D_6 , 25 °C) δ 116.6 (2 C, $\text{SiC}\equiv\text{C}^i\text{Bu}$), 79.3 (2 C, $\text{SiC}\equiv\text{C}^i\text{Bu}$), 74.8 (4 C, Cp), 74.1 (4 C, Cp), 68.0 (*ipso*-Cp), 31.0 (6 C, $\text{C}(\text{CH}_3)_3$), 28.5 (2 C, $\text{C}(\text{CH}_3)_3$); $^{29}\text{Si}\{^1\text{H}\}$ NMR (79.4 MHz, C_6D_6 , 25 °C) δ -46.0; GPC $M_n = 9.6 \times 10^3$, $M_w = 1.1 \times 10^4$, PDI = 1.15; UV-vis (25 °C, THF) $\lambda_{\text{max}} = 439$ nm, $\epsilon = 185$ $\text{L}\cdot\text{mol}^{-1}\cdot\text{cm}^{-1}$.

The above procedure was also used in molecular weight control experiments of PFS **3**, with irradiation times specified in Table 3.

Synthesis of 5. $\text{LiC}\equiv\text{CC}\equiv\text{CPh}$ (399 mg, 3.02 mmol) was dissolved in Et_2O (50 mL), and the solution was cooled to -35 °C. This was added dropwise to an Et_2O solution (50 mL) of **4** (798 mg, 3.04 mmol) at -50 °C. The reaction mixture was allowed to warm to 25 °C, and $(\text{CH}_3)_3\text{SiCl}$ (5 drops) was added. The red suspension was stirred for 20 min, and all volatile materials were removed in vacuo. After drying under high vacuum for 2 h, the orange residue was extracted with hexanes (4 \times 30 mL) and filtered through a glass frit to remove LiCl . The filtrate was concentrated to dryness to give an orange solid, which was recrystallized twice from toluene/hexanes (1:1) at -35 °C to give a red solid, yield 423 mg (40%). Crystals suitable for X-ray crystallography were grown by slow evaporation of a hexanes solution at 25 °C.

For **5**: ^1H NMR (400 MHz, C_6D_6 , 25 °C) δ 7.33–7.29 (m, 2 H, *ortho*-Ph), 6.89–6.82 (m, 3 H, *meta*- and *para*-Ph), 4.41–4.37 (m, 4 H, Cp), 4.36–4.32 (m, 2 H, Cp), 3.84–3.81 (m, 2 H, Cp), 0.49 (s, 3 H, CH_3); $^{13}\text{C}\{^1\text{H}\}$ NMR (100.5 MHz, C_6D_6 , 25 °C) δ 133.0 (Ph), 129.7 (*para*-Ph), 128.6 (Ph), 121.3 (*ipso*-Ph), 90.5, 85.9, 78.5, 75.1 ($\text{C}\equiv\text{CC}\equiv\text{CPh}$), 78.34, 78.26, 76.6, 74.4 (Cp), 29.1 (*ipso*-Cp), -3.4 (CH_3); $^{29}\text{Si}\{^1\text{H}\}$ NMR (79.4 MHz, C_6D_6 , 25 °C) δ -26.9; MS (EI, 70 eV) m/z (%) 352 (100); HRMS (EI, 70 eV) calcd for $\text{C}_{21}\text{H}_{16}^{56}\text{FeSi}$ 352.037068, found 352.038185, fit 3.2 ppm. Anal. Calcd for $\text{C}_{21}\text{H}_{16}\text{FeSi}$: C, 71.65; H, 4.58. Found: C, 71.38; H, 4.82; UV-vis (25 °C, THF): $\lambda_{\text{max}} = 482$ nm, $\epsilon = 300$ $\text{L}\cdot\text{mol}^{-1}\cdot\text{cm}^{-1}$.

Transition Metal-Catalyzed ROP of 5 Using Karstedt's Catalyst. **5** (50 mg, 0.14 mmol) was dissolved in toluene (1 mL), and Et_3SiH (11 μL , 0.069 mmol) and Karstedt's catalyst (5 μL) were sequentially added. The solution was stirred for 1 h 5 min, and it became slightly viscous and dark orange. Precipitation into dry hexanes gave a yellow powder, which were collected by filtration. Drying under high vacuum gave PFS **6**_{Karstedt's} as an orange solid, yield 25 mg (50%).

When this reaction was performed in the absence of Et_3SiH , a dark red solution was formed after 5.5 h with no increase in viscosity. Analysis of the reaction mixture by ^1H NMR and MS showed the presence of PFS **6** and the possible formation of the cyclic dimer of **5**.⁴⁹ Because the cyclic dimer of **5** could not be separated from PFS **6**, we were unable to obtain definitive characterization data.

For cyclic dimer of **5**: MS (EI, 70 eV) m/z (%) 704 (23), 84 (100).

For **6**_{Karstedt's}: ^1H NMR (400 MHz, C_6D_6 , 25 °C) δ 7.34 (d, $^3J_{\text{HH}} = 6.8$ Hz, 2 H, *ortho*-Ph), 6.98–6.90 (m, 3 H, *meta*- and *para*-Ph), 4.51, 4.41, 4.30, 4.26 (m, 8 H, Cp), 1.14–1.10 (CH_3CH_2 of end group), 0.88 (t, $^3J_{\text{HH}} = 6.8$ Hz, CH_3CH_2 of end group), 0.75 (s, 3 H, CH_3); $^{13}\text{C}\{^1\text{H}\}$ NMR (100.5 MHz, C_6D_6 , 25 °C) δ 133.0 (Ph), 129.5 (*para*-Ph), 128.6 (Ph), 121.7 (*ipso*-Ph), 89.9, 89.7, 78.4, 75.5 ($\text{C}\equiv\text{CC}\equiv\text{CPh}$), 74.6, 74.4, 74.3, 73.2, 73.1 (Cp), 68.3, 68.2 (*ipso*-Cp), 8.2, 7.8 (CH_3CH_2 of end group), 5.0, 3.4 (CH_3CH_2 of end group), -1.1 (CH_3); $^{29}\text{Si}\{^1\text{H}\}$ NMR (79.4 MHz, C_6D_6 , 25 °C) δ -22.1 (poorly resolved pseudotriplet); GPC analysis showed a bimodal distribution: peak 1, $M_n = 4.3 \times 10^6$, $M_w = 8.9 \times 10^6$, PDI = 2.05, 9%; peak 2, $M_n = 3.1 \times 10^4$, $M_w = 7.3 \times 10^4$, PDI = 2.35, 91%.

(49) The formation of a cyclic dimer has been previously observed in Karstedt's-catalyzed ROP without Et_3SiH , when a ferrocenophane with a phenylacetylide substituent was polymerized in THF. See ref 26 for details.

Transition Metal-Catalyzed ROP of 5 Using PtCl_2 to Give PFS **6 _{PtCl_2} .** **5** (50 mg, 0.14 mmol) was dissolved in toluene (1 mL), and Et_3SiH (11 μL , 0.069 mmol) was added to the solution with a microsyringe. A trace amount of PtCl_2 was then added, and the mixture was stirred for 2 h. The orange suspension was passed through a 0.45 μm syringe filter to remove Pt, and the solution was precipitated into dry hexanes (20 mL). An orange solid was isolated and washed with a small amount of hexanes and then dried overnight, yield 39 mg (78%).

For **6** _{PtCl_2} : ^1H NMR (400 MHz, C_6D_6 , 25 °C) δ 7.33 (d, $^3J_{\text{HH}} = 7.2$ Hz, 2 H, *ortho*-Ph), 6.90–6.83 (m, 3 H, *meta*- and *para*-Ph), 4.50, 4.40, 4.29, 4.25 (br s, 8 H, Cp), 1.14–1.04 (m, CH_3CH_2 of end group), 0.90–0.82 (m, CH_3CH_2 of end group), 0.75 (br s, 3 H, Me); $^{13}\text{C}\{^1\text{H}\}$ NMR (100.5 MHz, C_6D_6 , 25 °C) δ 133.0, 129.4 (*para*-Ph), 128.6 (Ph), 121.7 (*ipso*-Ph), 89.9, 89.7, 78.4, 75.5 ($\text{C}\equiv\text{CC}\equiv\text{CPh}$), 74.7, 74.6, 74.4, 74.3, 73.2, 73.1 (Cp), 68.3, 68.2 (*ipso*-Cp), 8.1, 7.8 (CH_3CH_2 of end group), 5.0, 3.4 (CH_3CH_2 of end group), -1.1 (Me); $^{29}\text{Si}\{^1\text{H}\}$ NMR (79.4 MHz, C_6D_6 , 25 °C): δ -22.1; GPC peak 1, $M_n = 3.8 \times 10^6$, $M_w = 6.9 \times 10^6$, PDI = 1.81, 15%; peak 2, $M_n = 4.0 \times 10^4$, $M_w = 1.2 \times 10^5$, PDI = 3.05, 85%.

Attempted Thermal ROP of 5 in Solution. **5** (165 mg, 0.47 mmol) was dissolved in mesitylene (1 mL), and the solution was heated at 180 °C. A solvent-swelling gel was obtained after 1 h.

This experiment was repeated with xylenes as solvent and heating at 160 °C. After 1 h 10 min, an orange solution and an orange gel were formed. Precipitation of the solution into ACS grade MeOH gave orange fibers. An orange solid was obtained after drying under high vacuum, yield 25 mg (15%). Its ^1H NMR spectrum contained peaks corresponding to PFS **6** only: ^1H NMR (400 MHz, C_6D_6 , 25 °C) δ 7.34 (br s, 2 H, *ortho*-Ph), 6.86 (br s, 3 H, *meta*- and *para*-Ph), 4.50, 4.41, 4.30, 4.26 (br m, 8 H, Cp), 0.75 (s, 3 H, Me); $^{13}\text{C}\{^1\text{H}\}$ NMR (100.5 MHz, C_6D_6 , 25 °C) δ 133.0 (Ph), 129.5 (*para*-Ph), 128.6 (Ph), 121.7 (*ipso*-Ph), 89.9, 89.7, 78.5, 75.5 ($\text{C}\equiv\text{CC}\equiv\text{CPh}$), 74.71, 74.67, 74.4, 74.3, 73.2, 73.1 (Cp), 69.32, 68.26 (*ipso*-Cp), -1.1 (CH_3).

Photocontrolled ROP of 5 to Give PFS **6_{PROP}.** In the absence of light, **5** (99 mg, 0.28 mmol) was dissolved in THF (ca. 2 mL) in a Schlenk tube. NaCp (2 M, 5.7 μL , 0.0114 mmol) was added, and the red solution was photolyzed at 5 °C for 2 h. The solution became orange and slightly viscous. Five drops of $(\text{CH}_3)_3\text{SiCl}$ was added to quench the polymerization, and precipitation into dry hexanes (20 mL) gave PFS **6**_{PROP} as an orange, gummy solid, yield 86 mg (87%).

For **6**_{PROP}: ^1H NMR (400 MHz, C_6D_6 , 25 °C) δ 7.33 (d, $^3J_{\text{HH}} = 7.6$ Hz, 2 H, *ortho*-Ph), 6.90–6.83 (m, 3 H, *meta*- and *para*-Ph), 4.50, 4.41, 4.30, 4.26 (br s, 8 H, Cp), 4.18 (br s, 5 H, Cp end group), 0.74 (s, 3 H, CH_3), -0.01 (s, 9 H, $\text{Si}(\text{CH}_3)_3$ end group); $^{13}\text{C}\{^1\text{H}\}$ NMR (100.5 MHz, C_6D_6 , 25 °C) δ 133.0 (Ph), 129.4 (*para*-Ph), 128.6 (Ph), 121.7 (*ipso*-Ph), 89.9, 89.6, 78.4, 75.5 ($\text{C}\equiv\text{CC}\equiv\text{CPh}$), 74.8, 74.7, 74.4, 74.3, 73.2, 73.1 (Cp), 68.33, 68.27 (*ipso*-Cp), -0.9 ($\text{Si}(\text{CH}_3)_3$ end group), -1.1 (CH_3); $^{29}\text{Si}\{^1\text{H}\}$ NMR (79.4 MHz, C_6D_6 , 25 °C) δ -22.1; GPC $M_n = 8.4 \times 10^3$, $M_w = 9.2 \times 10^3$, PDI = 1.10; UV-vis (25 °C, THF) $\lambda_{\text{max}} = 445$ nm, $\epsilon = 220$ $\text{L}\cdot\text{mol}^{-1}\cdot\text{cm}^{-1}$.

Synthesis of 7. 5 (100 mg, 0.28 mmol) and $[\text{Co}_2(\text{CO})_8]$ (200 mg, 0.58 mmol) were dissolved in toluene (2 mL) to give a dark brown solution. The solution was stirred at 25 °C for 2 h while vented to an oil bubbler to release evolved CO. All volatile materials were removed in vacuo to give a dark brown solid, which was recrystallized from toluene/hexanes (1:2) to give dark brown crystals, yield 160 mg (62%). Crystals suitable for X-ray crystallography were obtained from the same recrystallization.

For **7**: ^1H NMR (400 MHz, C_6D_6 , 25 °C) δ 7.72 (d, $^3J_{\text{HH}} = 7.2$ Hz, 2 H, *ortho*-Ph), 7.09 (t, $^3J_{\text{HH}} = 7.2$ Hz, 2 H, *meta*-Ph), 7.03–6.96 (m, 1 H, *para*-Ph), 4.47, 4.40, 4.35, 3.91 (br m, 8 H, Cp), 0.72 (s, 3 H, CH_3); $^{13}\text{C}\{^1\text{H}\}$ NMR (100.5 MHz, C_6D_6 , 25 °C) δ

199.7, 199.1 (CO), 138.7, 129.4, 129.3, 129.2 (Ph), 125.6, 99.8, 93.5, 79.7 (C(CO₂(CO)₆)C–C(CO₂(CO)₆)CPh), 78.5, 78.2, 76.2, 76.0 (Cp), 33.2 (*ipso*-Cp), –0.2 (CH₃); ²⁹Si{¹H} NMR (79.4 MHz, C₆D₆, 25 °C) δ –11.5; MS analysis was not possible, as the sample decomposed in the spectrometer. Anal. Calcd for C_{36.5}H₂₀Co₄FeO₁₂–Si·0.5C₇H₈: C, 45.19; H, 2.08. Found: C, 45.05; H, 2.14.

X-ray Crystallography. Selected crystal, data collection, and refinement parameters for **2**, **5**, and **7**·0.5C₇H₈ are given in Table 6. Single X-ray diffraction data were collected at 150(1) K using a Nonius Kappa-CCD diffractometer and monochromated Mo K α radiation ($\lambda = 0.71073$ Å). The data were integrated and scaled using the Denzo-SMN package.⁵⁰ The SHELXTL/PC package was used to solve and refine the structures.⁵¹ Refinement was by full-matrix least-squares on F^2 using all data (negative intensities included). Hydrogen atoms were placed in calculated positions and included in the refinement in riding motion approximations.

One of the *tert*-Bu groups in **2** was found to be positionally disordered over two sites. Initial refinement showed that the two

(50) Otwinowski, Z.; Minor, W. *Methods Enzymol.* **1997**, *276*, 307–326.

(51) Sheldrick, G. M. *SHELXTL/PC V 5.1*; Bruker Analytical X-ray Systems: Madison, WI, 1997.

components have equal occupancies, and the occupancies were fixed at 50% in the final refinement cycles. For **7**·0.5C₇H₈, one molecule of toluene was found to crystallize with two molecules of **7** in the lattice.

CCDC-626572 (**2**), CCDC-626573 (**5**), and CCDC-626574 (**7**·0.5C₇H₈) contain the supplementary crystallographic data for this paper. They can be obtained free of charge via the Internet at www.ccdc.cam.ac.uk/conts/retrieving.html.

Acknowledgment. W.Y.C. thanks the Natural Sciences and Engineering Research Council of Canada for a Canada Graduate Scholarship and the Walter C. Sumner Foundation for a fellowship. I.M. thanks the European Union for a Marie Curie Chair and the Royal Society for a Wolfson Research Merit Award.

Supporting Information Available: Supplementary crystallographic data for **2**, **5**, and **7** in CIF format. This material is available free of charge via the Internet at <http://pubs.acs.org>.

OM060767L